Acta Biomaterialia 69 (2018) 385–394

Contents lists available at ScienceDirect

Acta Biomaterialia

journal homepage: www.elsevier.com/locate/actabiomat

Full length article

Effect of strontium surface-functionalized implants on early and late osseointegration: A histological, spectrometric and tomographic evaluation

Vincent Offermanns [a,*], Ole Z. Andersen [b], Gregor Riede [a], Michael Sillassen [b], Christian S. Jeppesen [c], Klaus P. Almtoft [c], Heribert Talasz [d], Caroline Öhman-Mägi [e], Bernd Lethaus [f], Rene Tolba [g], Frank Kloss [h], Morten Foss [b,i]

[a] Department of Cranio-, Maxillofacial and Oral Surgery, Medical University Innsbruck, Austria
[b] Interdisciplinary Nanoscience Center (iNANO), Faculty of Science and Technology, Aarhus University, Denmark
[c] Tribology Centre, Danish Technological Institute, Aarhus, Denmark
[d] Biocenter, Division of Clinical Biochemistry, Medical University Innsbruck, Austria
[e] Materials in Medicine, Division of Applied Materials Science, Department of Engineering Sciences, University Uppsala, Sweden
[f] Department of Cranio-, Maxillofacial and Oral Surgery, RTWH Aachen, Germany
[g] Central Laboratory Animal Facility, RTWH Aachen, Germany
[h] Private Practice, Lienz, Austria
[i] Department of Physics and Astronomy, Faculty of Science and Technology, Aarhus University, Denmark

ARTICLE INFO

Article history:
Received 23 October 2017
Received in revised form 18 January 2018
Accepted 30 January 2018
Available online 7 February 2018

Keywords:
Biofunctionalization
Bone
Osteoinduction
Release
Dental
Orthopedic

ABSTRACT

Numerous *in vivo*, *in vitro* and clinical studies report on beneficial effects of strontium with respect to increased bone growth. Based on this knowledge the aim of this study was to evaluate early and late osseointegration stages of functionalized titanium implants showing sustained release of strontium (Sr) and further investigate its potential systemic effect.

Strontium functionalized (Ti-Sr-O) and Grade 4 (Control) titanium implants were inserted in the femoral condyle of New Zealand White rabbits. The Ti-Sr-O coating was characterized using Scanning Electron Microscopy (SEM) and Energy Dispersive X-ray Spectrometry (EDX) for structure, coating thickness and chemical composition. Inductively Coupled Plasma Atomic Emission Spectrometry (ICP-AES) was used to evaluate released strontium *in vitro* while Atomic Absorption Spectrometry (AAS) was utilized to monitor serum levels of strontium and calcium. Additionally, histological and tomographic analysis of bone-to-implant contact (BIC%) and bone formation (BF%) was performed, following implantation periods of two or twelve weeks, respectively.

Median values for BIC% for Ti-Sr-O revealed significant differences within the two- and twelve-week observation periods, while exceeding BF% was discovered especially after twelve weeks when performing the histological evaluation. The results from the micro-computed tomography (μ-CT) showed no significant differences, when comparing the experimental groups. AAS measurements did not indicate a systemic effect by the local strontium release.

Within the limitations of the study, it was shown that a Ti-Sr-O coating with sustained release characteristics of strontium, accelerates bone apposition and represents a potential potent surface modification for endosseous medical implant devices.

Statement of Significance

This study presents first data with respect to early and late *in vivo* response on a strontium functionalized titanium surface comprising a nanotopography manufactured by a magnetron sputtering process. We investigated different osseointegration stages of screw-shaped implants with dental implant geometries in a rabbit femur model observing beneficial effects of the functionalized surface on bone-to-implant contact and bone formation caused by tailored release of the bone anabolic strontium. Histomorphometrical data revealed that a functionalized titanium surface with controlled liberation of strontium accelerates

* Corresponding author.
E-mail address: vincent.offermanns@i-med.ac.at (V. Offermanns).

https://doi.org/10.1016/j.actbio.2018.01.049
1742-7061/

osseointegration while spectrometry measurements did not indicate a potential systemic effect of this osteoinductive agent and could thus have impact on modifications of medical implant devices.

1. Introduction

Osseointegration is a crucial factor for long-term stability of bone anchored implants and thus represents a decisive aspect for successful treatment in relation to orthopedic and oral rehabilitation [1,2]. The material of choice for manufacturing of dental and orthopedic implant devices is titanium. Due to the forming of a nanometer thick native oxide at the surface of the implant, the surface is passivated leading to chemical inertness and good mechanical behaviour. In order to further improve the performance, numerous evaluations of physical, chemical and biological modifications of titanium implants for enhancing osseointegration has been carried out [3–7]. Investigations performed using defined study populations have revealed satisfying results of endosseous implant devices [1,2,8]. Nonetheless, with a growing aging population, different challenges e.g. diminished bone conditions due to irradiation or osteoporosis remain. This led to continuative research in animal models, however, with a lack of clinical application of developed functionalized medical devices. Today, defined geometrical properties and surface characteristics with e.g. implementation of bioactive ions, standardized insertion and loading protocols for specific clinical applications [3,5,9,10] assure predictable results. Parallel to these advances, research has provided several experimental modifications with e.g. BMP-2, calcium (Ca), magnesium (Mg) or strontium (Sr) to enhance bone regeneration and osseointegration [11–14]. Furthermore, functionalized surfaces are required to maintain their osteogenic properties and surface characteristics since defined macro-, micro- or nanostructure promotes e.g. protein absorption and adhesion of monocytes to a certain extent contributing to the crucial steps of osseointegration [15–17]. Implant topography within the submicron scale, with incorporated strontium in particular, could have possible impact on surface modification affecting both microbial attachment and bone anchorage [18–22]. Since the first medical report on strontium administration as osteoporotic treatment in the 1950's [23], the alkali earth metal and trace element faded into the spotlight of research with consecutive clinical investigations reporting on anabolic effects with respect to bone metabolism [24–26]. The exact molecular mechanism remains unclear, however, interference in the RANK/RANKL/OPG pathway has been demonstrated, as well as activation of different Wnt pathways and stimulation of the calcium sensing receptor leading to increased osteoblastic activity [27]. Additionally, MSC differentiation towards the osteogenic lineage was observed *in vitro* [28]. The incorporation of strontium in glasses, cements or titanium surfaces as osteoinductive factor is a proven concept [29–32], recently also with tailorable strontium released into the *peri*-implant tissues [14,33].

Based upon the knowledge on the beneficial effect of strontium on bone ingrowth at the bone-implant interface, reported in the literature as well as data gained from previous rodent studies of our group [14,33,34], this study presents the evaluation of a functionalized titanium surface with continuous release of strontium. The Ti-Sr-O coating has been manufactured by using an industrial-scale magnetron sputtering process. Chemical composition, morphology and strontium release were assessed pre-operatively. While utilizing an established rabbit femur model for implant insertion [35], spectrometric measurements of blood samples were conducted to determine both strontium and calcium levels. Moreover, histological sectioning as well as micro-computed tomography was performed after two and twelve weeks healing periods.

The aim of the study was to evaluate early and late osseointegration patterns of a strontium-modified surface with surveillance of possible systemic impact by the functionalized surface. Results indicate that Ti-Sr-O surfaces, showing tailored release profile of strontium, contribute significantly to enhanced bone healing and could become a potential candidate for surface modification in dental and orthopedic implantology.

2. Material and methods

2.1. Sample preparation

Test implants, measuring 8 mm in length with an outer maximum diameter of 3.75 mm, were manufactured from Grade 4 titanium (Elos Medtech Pinol A/S, Gørløse, Denmark). The implants had a turned surface finish. At this point, two groups were established; I) unmodified titanium implants (Ti) and II) implants with Ti-Sr-O coating. The Ti-Sr-O coating was deposited onto the Ti implants by non-reactive DC magnetron sputtering using an industrial-scale sputtering system, as previously described [14,36]. In brief, substrates were mounted on a rotating sample stage with Grade 1 Ti and a sintered composite $SrTiO_3$, used as targets. All components comprised purities of 99.9%. The two targets had a size of $88 \times 500\ mm^2$ with application of a defined relative target power and a chamber pressure of 1 mPa Argon used as sputtering gas. No substrate heating was employed during the deposition.

2.2. Sample characterization

Implants from the Ti-Sr-O group were examined using Scanning Electron Microscopy (SEM, Nova 600, FEI Company, Netherlands) to allow for evaluating the structure and thickness of the coating. To assess the coating thickness implants were embedded in a conducting resin (PolyFast, Struers, Denmark) and subsequently processed to allow for obtaining a cross-sectional view of the coating. In short, sample processing involved initial planarization of the sample by grinding, using a grid size of 220. Subsequently, polishing of the surface was performed in three steps, initially using a suspension of abrasive particles of 9 μm in size, going down to 3 μm and, finally 1 μm (DiaPro 9, 3 and 1, Struers, Denmark). The thickness was measured at various positions, using the measuring tool of the SEM software. The SEM is fitted with an Energy Dispersive X-Ray Spectrometer (EDX, EDAX, AMETEK, Meerbusch, Germany), which was used to examine the chemical composition of the coating at three different positions at the implant surface (flat part, edge and bottom of thread). For the analysis an acceleration voltage of 20 kV was utilized.

2.3. Strontium release

The release of strontium from the Ti-Sr-O modified implants was assessed by performing washout series in Phosphate Buffered Saline (PBS) at pH 7.4. More specifically, a total of five implants

were each immersed in 1 ml of PBS. To prevent liquid from being retained within the internal geometry of the implants, the end of the implants was sealed off using implant healing caps (Elos Medtech Pinol A/S, Gørløse, Denmark). The immersed implants were incubated at 37 °C under static conditions, initially for a period of one day. At this point, all liquid was collected from the vessels containing the implants and stored for later analysis. Following this, 1 ml of fresh PBS was added to each of the implants and the incubation period was continued. Additional samples were collected, using the same procedure, at day 3, 5, 7, 14, 28, 42, 56 and 84 (week 12). When all samples had been collected, these were analyzed using Inductive Coupled Plasma Atomic Emission Spectroscopy (ICP-AES, Optima 3300 DV, Perkin-Elmer, MA, USA) [34].

2.4. Surgery

After permission of the governing authority (LANUV 84-02.04.2013.A469) and the local ethics committee, 36 nine month old, male New Zealand White Rabbits (weight 4500 g) underwent surgical procedure in accordance with the ARRIVE guidelines [37]. Animals were held in a room with a 12 h:12 h light:dark cycle with room temperature of 18–20 °C. Rabbits were individually housed and were fed ad libitum with appropriate pellets (V2333, ssniff® K-H, Ssniff, D-59,494 Soest, Germany) while tap water was available ad libitum by an automatic drinking system. For surgical procedure animals were randomly chosen with insertion of either; I) one coated implant (Ti-Sr-O) and one titanium implant (Ti) or II) two titanium implants (Control). By using Ti twice, an actual control without any potential bias from the strontium releasing surface Ti-Sr-O with respect to histomorphometry and blood serum analysis is provided. Thus, each animal was carrying two implants, one in each femur (animals per time point with Ti-Sr-O/Ti n = 12; animals per time point with Ti/Ti n = 6). In more detail, the surgical procedure was performed as follows: after a two week settling-in period animals were anesthetized with Medetomidine (Domitor® 1 mg/ml; 0.2 ml) and Ketamine (Ketavet® 100 mg/ml; 0.2 ml) intravenously. After shaving and disinfection, a 20 mm incision was made medial to the patella with subsequent preparation and thrusting aside of the patellar tendon. The implant bed in the distal part of the femur was prepared by drilling, using ascending drill diameters. The size sequence was pre-drill, 2.2 mm, 3.3 mm and profile drill. All steps were performed while cooling the operation site with isotonic saline solution (Sigma-Aldrich, Schnelldorf, Germany). The utilized implants had a self-tapering design, thus, implant insertion was performed immediately after preparation of the implantation site. Soft tissue closure was performed with Vicryl 4–0 (Ethicon, Johnson & Johnson Medical GmbH Norderstedt, Germany). Overview of the surgical procedure and a radiographic image of the implant position is presented in Fig. 1. Postsurgical treatment included analgesic as well as antibiotic treatment, administered by subcutaneous injections with Carprofen (Rimadyl® 4 mg/kg BW) and Enrofloxacin (Baytril® 7.5 mg/kg BW). After the pre-determined periods (two weeks n = 18; twelve weeks: n = 18), animals were euthanized with intravenous application of Narcoren® (Pentobarbital 400 m g/kg BW).

2.5. Atomic absorption spectrometry (AAS)

Blood samples of approximately 1.5 ml were taken preoperatively and on day 1, 3, 5, 7, 14, 21 and 28 post-surgery. The procedure was conducted after guidelines of GV-SOLAS [38]. Strontium in serum was analyzed using a Zeeman atomic absorption spectrometer M6, equipped with a graphite furnace GF95Z and a furnace autosampler FS95 (all from Thermo Fisher Scientific) at 460.7 nm (graphite furnace atomic absorption spectrometry GF-AAS). Extended lifetime graphite cuvettes (Thermo Fisher Scientific) were used for the longitudinally heated atomizer with argon as inert gas at a constant flow of 0.2 L/min throughout the heating program, except during the atomization step, when the gas flow was interrupted. A pyrolysis temperature of 1000 °C and an atomization temperature of 2800 °C were used. Zeeman background correction was employed to compensate for non-specific absorption. The calibration solutions (0.25 μg/L to 5 μg/L) were prepared by adequate dilution of a 1000 mg/L strontium standard (Fluka, Sigma-Aldrich) stock solution with 0.1% ultrapure nitric acid (Merck), 0.1% Triton-X100 (Sigma-Aldrich) and high-purity water (Milli-Q system, Millipore). Serum samples were diluted 20 fold in 0.1% ultrapure nitric acid, 0.1% Triton-X100, prior to analysis. Calcium in serum was determined using a Thermo M6 flame

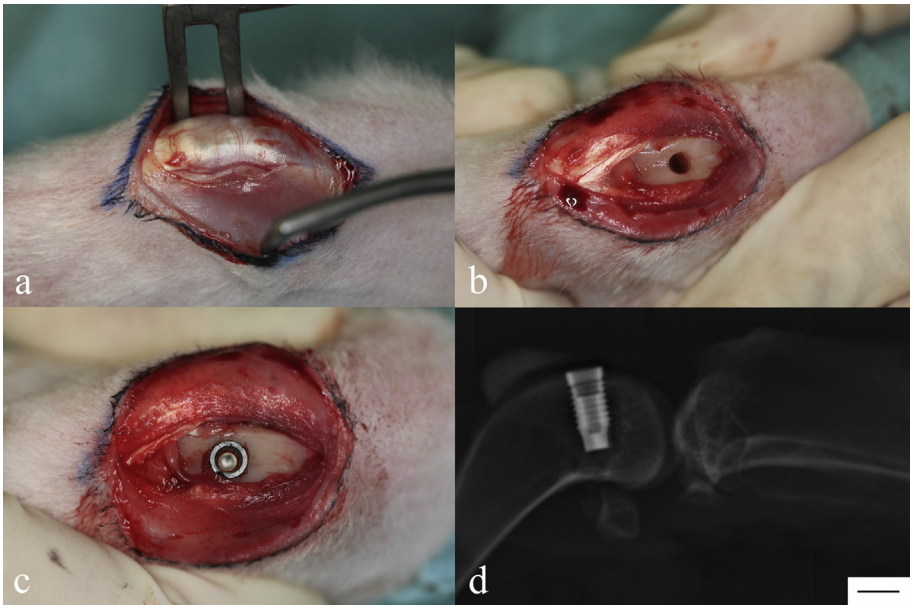

Fig. 1. a) surgical site with exposed patellar ligament, b) femoral condyle with prepared implant bed, c) inserted implant, d) conventional X-ray showing the implant in the femoral condyle. Scale bar in the lower right section is 4 mm.

atomic absorption spectrometer in a nitrous oxide-acetylene (4.5 L/min) flame at 422.7 nm. The calibration solutions (0.1 mg/L to –1 mg/L) were prepared by adequate dilution of a 1000 mg/L calcium standard Titrisol (Merck) stock solution with 0.1% hydrochloric acid and 0.2% potassium chloride as ionization solution. Serum samples were diluted 200 or 400 fold with 0.1% hydrochloric acid, 0.2% potassium chloride solution.

The accuracy of the strontium and calcium measurements was assessed through the analysis of lyophilized control samples Seronorm Trace Elements Serum (Sero AS) which were reconstituted according to the manufacturer's instruction with Milli-Q water and further diluted, using the same approach as for the serum samples. Interassay coefficient of variance (CV) was <5.5% and intraassay CV <2%. Values for the standard serum concentration was 30 μg/L for strontium and 2.4 mmol/L for calcium, respectively.

2.6. μ-CT

Following euthanization, *peri*-implant soft and hard tissue were harvested. Prior to embedding, to allow for visualizing of the orientation of the implants in the femur, individual PEEK-guide pins were mounted into the internal geometry of the implants. Subsequently, all specimens were embedded in Technovit 9100 new® (Heraeus Kulzer Austria GmbH, Nordbahnstraße, Vienna, Austria), according to the manufacturer's manual. The embedded samples were scanned by micro-computed tomography (SkyScan 1172, Bruker microCT, Kontich, Belgium) at a voltage of 100 kV and a current of 100 μA, with a Cu-Al filter. Images were acquired using an isotropic pixel size of 7.9 μm. Reconstruction of cross-sections was done using software package NRecon (Bruker microCT, Kontich, Belgium). Software package DataViewer (Bruker microCT, Kontich, Belgium) was used to align the specimens. For each sample, at a distance of 2.6 mm from the top (at the first thread), a stack of 381 consecutive cross-sections (corresponding to a height of 3 mm) were analyzed. Three different volumes of interest (VOI) were used: inside the thread (VOI-I); 250 to 500 μm outside of the thread (VOI-II) and from 500 μm to 1.5 mm outside of the thread (VOI-III), as seen in Fig. 2. Bone volume fraction (BV/TV) was calculated for all three VOIs, while trabecular thickness, trabecular separation and trabecular number was calculated only for VOI-III. Bone-to-implant contact (BIC) was calculated as the bone volume fraction in a 2-voxel-thick VOI that excludes the 6 voxels (i.e. 50 μm) closest to the surface due to metal artefacts from the titanium screw. Osseointegration volume per total volume (OV/TV) was used as a 3D of bone-to-implant contact.

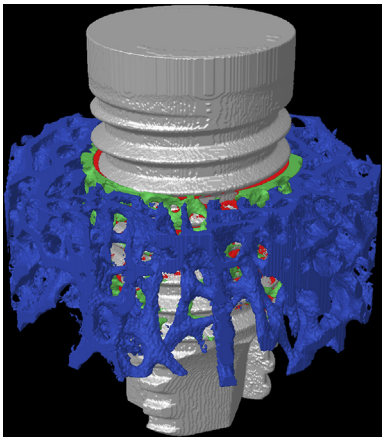

Fig. 2. Volumes of interests (VOI) investigated with micro-computed tomography; red: inside the thread (VOI-I); green: 250 to 500 μm outside of the thread (VOI-II); blue: from 500 μm to 1.5 mm outside of the thread (VOI-III).

2.7. Histomorphometrical analysis

Histological processing was conducted with the method described by Donath und Breuner [39]. In brief, Technovit blocks were glued on glass slides and cut along the long axis of the implant using a bandsaw (Exakt 300, Exakt, OK, USA). Following the initial sectioning, the freshly cut surface was glued to a new microscope slide, to allow for secondary cutting. Subsequently, grinding was performed using abrasive paper with a grit size of 1000, 2000 and 4000 to yield samples with a thickness of 50 μm. Finally, polishing was conducted using Micropolish 2.0 (Buehler, Germany). Toluidine blue staining was applied as a final procedure, to prepare the samples for image acquisition, which was performed using a Nikon Eclipse 80i microscope (Nikon GmbH, Austria). Bone formation and bone-to-implant contact was assessed at 40x magnification, using the software NIS Elements BR 3.10 (Nikon GmbH, Austria). Regions of interest (ROI) were determined as ROI-I, 0–250 μm (inside the thread of the implant) and ROI-II 250–500 μm (outside the thread of the implant). Using the defined ROI, data was expressed as area percentage of bone formation (BF%); bone-to-implant contact BIC% was evaluated as direct contact between bone and the implant surface (Fig. 3). Two slides per implant with two areas for evaluation on either side of the implant were used with all measurements taken within the spongy part of the femur.

2.8. Statistical analysis

Analysis for statistical significance in relation to the *in vitro* tests was performed using Students *t*-test while *in vivo* experiments were evaluated with Mann-Whitney *U* test; for all experiments a P-value of < 0.05 was considered statistically significant. *In vitro* data are presented as mean ± standard deviation while *in vivo* data are shown as median ± interquartile range as a matter of sample quantity. Statistical analysis was performed using SPSS for Windows® 15.0.1 (SPSS, Inc., Chicago, IL) and Microsoft Excel 2010 (Microsoft Corporation, Redmond, WA).

3. Results

All 36 animals completed the study as planed with either a two-week or a twelve-week observation period. Apart from the expected swelling around the knee joint, healing was uneventful in all animals; no complications such as infections, wound dehiscence or allergic reactions were observed throughout the study period. Moreover, no premature exposure or loss of inserted implants was detected.

3.1. Sample characterization

SEM was performed to evaluate the surface structure of the coating applied to the implant geometries. Fig. 4 presents the observed surface structure and cross-sectional view of the coating, the latter acquired from an embedded implant. As known from previous investigations, the surface roughness of the Ti-Sr-O functionalization is within the nanometer range [34] while the Grade 4 titanium implant represents a turned surface finish. As is evident from the images, a nanometer sized cauliflower-like structure is observed.

By using the embedded implant, it was possible to visualize and measure the coating thickness on different positions on the implant as seen in Table 1 and shown in Fig. 5, respectively. Since the deposition process is a line-of-sight evaporation process, the coating thickness varies on a complex substrate geometry due to shadowing effects. This explains the slightly lower thickness in the bottom of the thread.

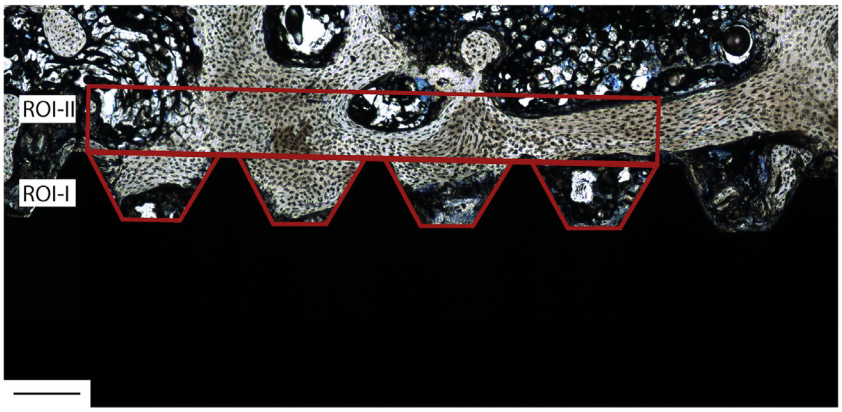

Fig. 3. Evaluation of bone formation BF% in ROI-I 0–250 μm, ROI-II 250–500 μm (red markings inside and outside the thread). The area of bone apposition was measured for all samples and used to calculate the percentage of de novo bone synthesis with respect to the total reference area. Bone-to-implant contact BIC% was measured directly at the implant interface and expressed as ratio to the total length. Scale bar is 250 μm.

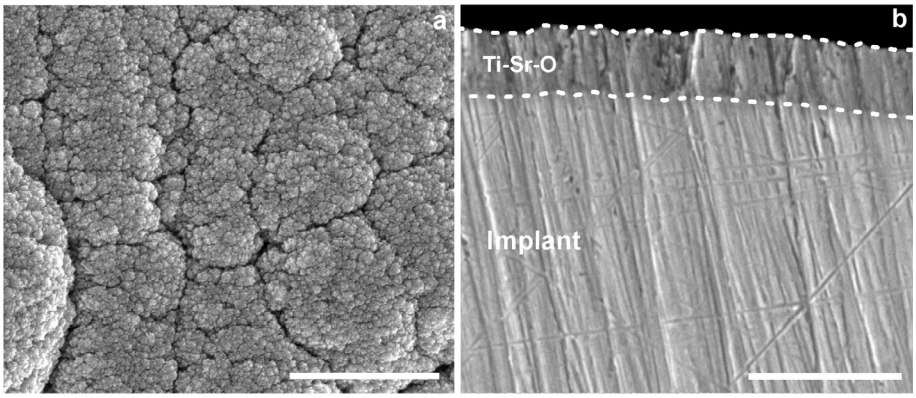

Fig. 4. a) Top view SEM of the Ti-Sr-O coating. The coating is characterized by a cauliflower-like nanostructure. b) Representative SEM image showing a cross-sectional view of the Ti-Sr-O coating acquired from an embedded implant. The thickness of the Ti-Sr-O coating is highlighted by the dotted lines. Scale bar is a) 1 μm, b) 5 μm.

Table 1
Coating thickness as measured using SEM. It is evident that the geometry of the implant influences the thickness of the deposited coating. The bottom of the thread shows a lower average thickness compared to that found for the area at the top of the screw thread and the flat area.

Location	Coating thickness [μm]
Flat area	1.8 ± 0.2
Edge of thread	1.5 ± 0.2
Bottom of thread	1.4 ± 0.1

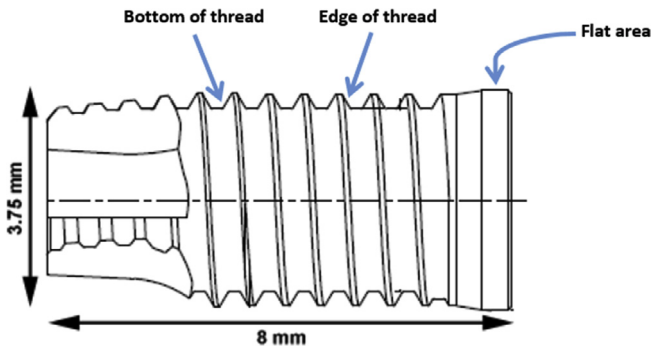

Fig. 5. Schematic drawing of manufactured implants and investigated coating thickness in areas of interest.

EDX was used to evaluate the chemical compositions of the Ti-Sr-O coating. Table 2 presents the average values acquired at the three different positions on the implant content of strontium, oxygen and titanium. Since especially the oxygen content is difficult to quantify accurately by EDX, the chemical compositions were verified on coated witness samples by X-ray photoelectron spectroscopy (XPS) and Rutherford Backscattering Spectroscopy (RBS), as previously described [36]. Data for the current study is included in supplementary material.

3.2. Strontium release

Strontium release was determined through examining the *in vitro* release by analyzing the amount of strontium in the wash-out buffer. The analysis was performed using ICP-AES and the results are presented in Fig. 6.

Table 2
Chemical composition of the Ti-Sr-O surface as determined by EDX. The data was collected from three geometrically distinct positions at the surface of the implant. The chemical composition was found to be similar at all positions.

Location	Titanium [at.%]	Strontium [at.%]	Oxygen [at.%]
Flat area	33.7	7.4	59.0
Edge of thread	28.4	6.2	65.4
Bottom of thread	29.6	6.4	64.0
Average % ± STD	30.6 ± 2.8	6.7 ± 0.6	62.8 ± 3.4

3.3. Blood serum content of strontium and calcium

Atomic absorption spectrometry (AAS) was utilized to analyze the blood serum concentration of strontium and calcium from day 0 to day 28 (Fig. 7). For the majority of time points constant strontium concentrations were observed similar to the level before surgical procedure, however, at day 14 a transiently increased content was found. At day 21 and 28, the concentration had returned to the initial level. Except for this maximum value, the strontium level was approximately 60 μg/L. Calcium levels revealed values between 2.5 and 3.5 mmol/L throughout the period.

3.4. μ-CT

Median and interquartile ranges for the bone volume fraction in the three different VOIs, two and twelve weeks after surgery, are presented in Table 3. Although a trend of more bone in Ti-Sr-O, especially within the threads (VOI-I), could be noticed at two weeks, no significant difference could be found between the groups. Twelve weeks after surgery, the Control group was found to have a statistically significantly higher bone volume fraction compared to Ti-Sr-O (in all three VOIs) and Ti (in VOI-I and VOI-III). Moreover, the trabecular thickness and trabecular number (calculated in VOI-III) was found to be larger in Control compared to Ti-Sr-O and Ti twelve weeks post-operatively (see Table 3). Subsequently, the trabecular separation was also smaller in the Control group compared to Ti-Sr-O after twelve weeks. At two weeks, no difference among the groups was found. Additionally, osseointegration volume over total volume is presented in Table 3. No statistically significant differences were found, neither between groups nor time points. However, at two weeks a trend of more bone in Ti-Sr-O and Ti compared to Control was observed.

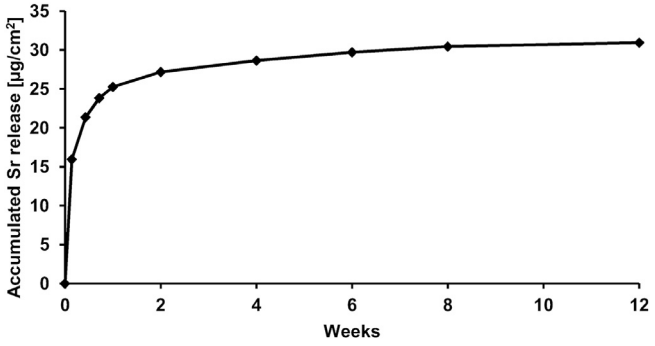

Fig. 6. Accumulated strontium release determined by ICP-AES analysis of washout buffer solutions. It is evident that the majority of strontium is liberated within the first two weeks, however, the release is found to be sustained over the full time period of the experiment, though at a lower rate. Data is shown as mean ± standard deviation.

3.5. Histomorphometrical analysis

Fig. 8 shows exemplary slides for the two and twelve week group of all investigated groups with zoomed images of analyzed areas below the associated experimental group. Fig. 9 presents results of BIC% with median ± interquartile ranges. Two and twelve weeks after surgery, Ti-Sr-O showed statistically significant differences compared to Ti and Control. Analysis of the two time periods showed also disparities of Ti and Control but not for Ti-Sr-O.

Results of new bone formation in ROI-I and II are shown in Fig. 10 and Fig. 11, respectively. For the two-week period Ti-Sr-O revealed significant differences compared to both other groups in ROI-I while in ROI-II the Control group was significantly lower than Ti and Ti-Sr-O. The Control group showed increased values in ROI-I and II following a twelve-week time frame. Moreover, differences within the groups comparing the two time intervals, were significantly more perceptible in the Control group. Significant increase for BIC% was observed comparing the two time intervals except for Ti-Sr-O; significant differences were seen in all investigated groups within ROI-I while Ti and Ti-Sr-O showed almost no disparities with respect to ROI-II regardless of the healing time.

4. Discussion

Research on improvement of osseointegration is growing due to more complex cases, challenging clinical situations and, not least, because of higher patient demands both in orthopedic and dental implantology. While systemic treatment with strontium ranelate (SrRan) divulged substantial advantages for patients with impaired bone metabolism [24,40] it has also been found to be effective for increasing *peri*-implant bone formation in animal models [41,42]. Research from our group also found beneficial results for Ti-Sr-O modified implant surfaces in previous rodent studies [14,33,34].

In the current study, histomorphometrical analysis showed superior findings of the strontium-functionalized surface with respect to BIC% at both two- and twelve-week time intervals. This is noteworthy since BIC% is considered as gold standard for evaluation of bone apposition around metallic implants with a great consensus that contact osteogenesis is responsible for successful

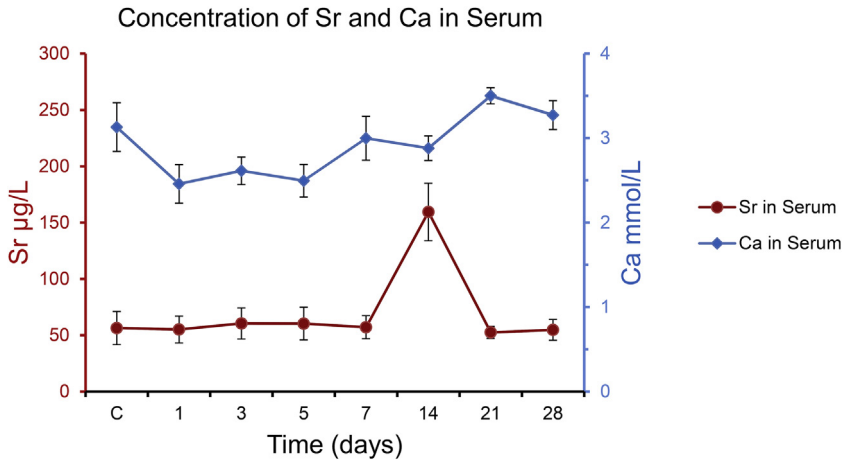

Fig. 7. Concentrations of strontium and calcium in serum of rabbits were measured with GF-AAS before (C) and 1 to 28 days after the surgical procedure. The elevated strontium level at day 14 was confirmed by repeated measurements. Data is presented as mean ± standard deviation.

Table 3
Analysis shows comparison of bone volume to total volume BV/TV (%) in standardized volumes of interest (VOI-I, II and III) as well as trabecular thickness Tb. Th (μm), trabecular separation Tb. Sp (μm) and trabecular number Tb. N (mm^{-1}). Additionally, osseointegration volume over total volume OV/TV (%) is stated. Data presented with median ± interquartile ranges.

Parameters	Control		Ti		Ti-Sr-O	
	2 weeks	12 weeks	2 weeks	12 weeks	2 weeks	12 weeks
BV/TV (%) – VOI-I (inside the thread)	48.7 (37.5–53.8)	63.8 (61.1–67.5)	56.7 (53.2–61.6)	55.4 (50.0–59.0)	62.1 (57.0–67.6)	57.2 (51.4–59.1)
BV/TV (%) – VOI-II (250 to 500 μm outside of the thread)	36.5 (26.7–41.9)	47.3 (43.8–53.7)	42.5 (34.0–46.8)	37.7 (33.4–51.2)	41.7 (39.3–44.3)	36.2 (34.6–43.0)
BV/TV (%) – VOI-III (from 500 μm to 1.5 mm outside of the thread)	26.5 (21.4–31.5)	36.6 (31.5–39.0)	33.4 (30.5–35.9)	27.7 (22.0–33.5)	35.2 (34.7–37.4)	23.3 (21.5–29.2)
Tb. Th (μm) – VOI-III	174 (167–191)	220 (200–230)	196 (184–215)	195 (176–206)	195 (188–207)	168 (152–198)
Tb. Sp (μm) – VOI-III	567 (519–577)	511 (477–550)	525 (484–566)	622 (482–696)	488 (433–585)	599 (550–668)
Tb. N (mm^{-1}) – VOI-III	1.43 (1.32–1.61)	1.61 (1.48–1.72)	1.72 (1.48–1.76)	1.40 (1.15–1.69)	1.92 (1.60–1.95)	1.33 (1.25–1.46)
OV/TV (%)	55.1 (42.7–55.9)	58.6 (49.1–70.9)	56.0 (52.4–60.3)	59.0 (55.4–63.8)	57.8 (54.8–58.7)	57.2 (51.0–60.3)

treatment in implant therapy [7,43–45]. The resembling values seen for Ti-Sr-O with respect to BIC% after two and twelve weeks were interpreted as acceleration of bone healing which could be advantageous in complex clinical situations while *peri*-implant bone formation expressed similar results after both time intervals, particularly in ROI-II. Those results emphasize the hypothesis of a local near-surface effect of strontium released in situ directly at the implant-tissue interface, since no significant differences could be observed 250–500 μm away from the surface.

The utilized titanium implants of representative sizes for dental applications were functionalized with the previously used industrial-scale magnetron sputtering process comprising nanostructured thin coatings [14,34] and subsequently tested in an established rabbit femur model [35]. In contrast to preceding experiments [14,33,34], the current study was performed in a larger animal model in order to insert implants of dental implant geometries. With a view to a potential systemic effect of released strontium from the functionalized titanium surface, blood samples were analyzed with atomic absorption spectrometry. Additionally, micro-computed tomography was conducted. Concerning the previously established evidence that systemic treatment with SrRan increases the risk for developing health related issues, like cardiovascular or thrombotic events [46], this points towards caution with respect to using strontium for accelerating the osseointegration process. However, comparing the amount of strontium released from the surface of the implants to the estimated daily intake of strontium of ~4 mg/day [47] found for patients, the risk associated with the current Ti-Sr-O technology has to be considered negligible. An eventual local cytotoxic effect was investigated earlier, with no indication of cytotoxic effects since cellular viability did not correlate with the strontium release [14]. Thus, the potential benefits on skeletal impairment when it comes to acceleration of osseointegration by local release kinetics in relation to bone anchored implants outweigh the potential risks.

Based on the findings of the current study, a constant in situ release of strontium could have the capability to show a clinical effect, without having the risk of the exceeding concentration in other tissues and blood, reaching a critical value over extended periods of time. It should be noted that the strontium release will most likely depend on the choice of fluid. In this study PBS was chosen as buffer. In the case of serum or a simulated body fluid, high concentrations of ions are already present, and apatite formation may influence the free ion concentrations as well. This dependence has previously been observed for ion release from bioactive glasses [48]. Thus, the release in an *in vivo* situation may differ from the *in vitro* ICP-AES data.

Bone properties are benefitting by local administration of this osteogenic element [49] and were evaluated in various experimental set-ups [30,32,50,51]. For the current study, to provide data of a potential systemic distribution of released strontium, serum analysis with atomic absorption spectrometry revealed constant levels of both investigated elements (strontium and calcium) with the exception of day 14 where strontium peaked to maximum value of 160 μg/L. It is noticeable that pronounced values of strontium on day 14 were also observed in rabbits carrying two times Ti (Control) while the increase was transient since the base level was reached again on day 21. Due to multiple measurements, an experimental artifact is ruled out and the strontium increase interpreted as mobilization of strontium from bone as a consequence by de- and remineralization. Osteoblasts first deposit unmineralized osteoid and release mineral-nucleating proteins that catalyze the process where osteoid starts to calcify, which occurs after approximately 15 days [52]. The observed peak might also be linked to faster bone remodeling in rabbits [53] since a large portion of strontium is released within the first three days after insertion [14] and hence unlikely a direct result of the functionalized sur-

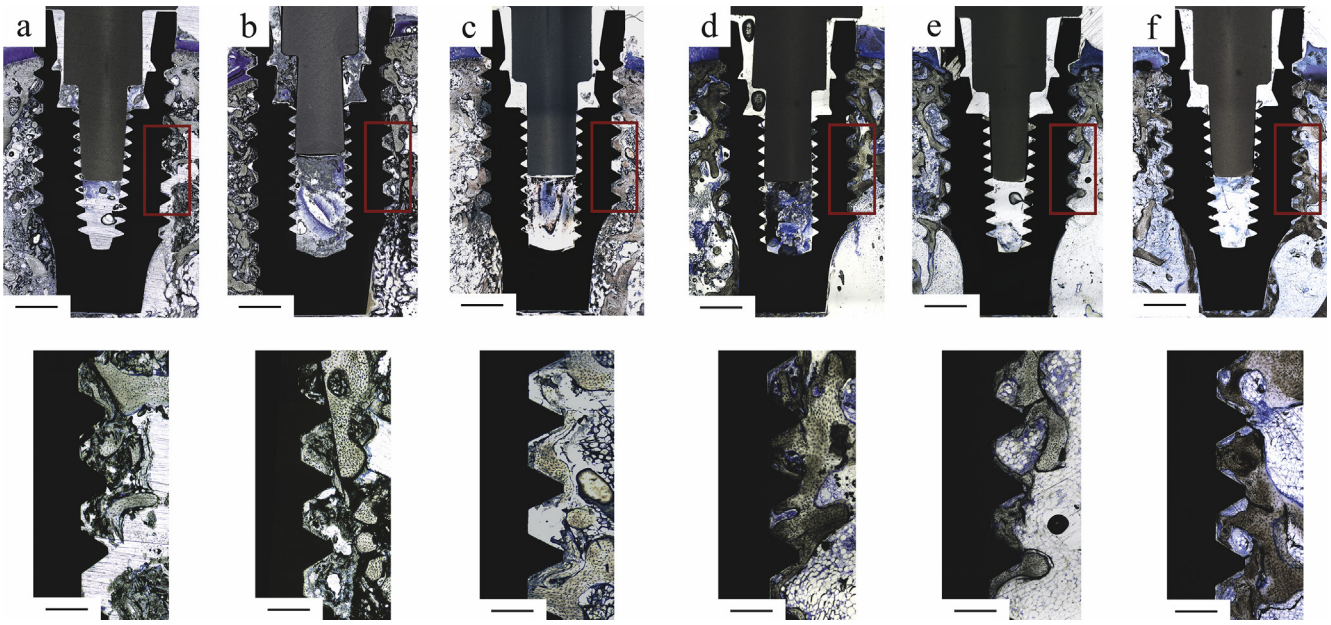

Fig. 8. Histological samples, stained with toluidine blue, with zoomed sections of regions of interest. Red box indicates the standard area used to evaluate new bone formation in the cancellous bone of the femur. a) two weeks, Control b) two weeks, Ti c) two weeks, Ti-Sr-O; d) twelve weeks, Control e) twelve weeks, Ti e) twelve weeks, Ti-Sr-O. The area of new bone formation was measured for all samples and used to calculate the percentage of de novo bone synthesis with respect to the total reference area in ROI-I and II. Direct bone contact to the implant surface with respect to the total length of the reference was subjected as bone-to-implant contact. Scale bar is 1000 μm in the upper total section and 300 μm in the lower zoomed segment.

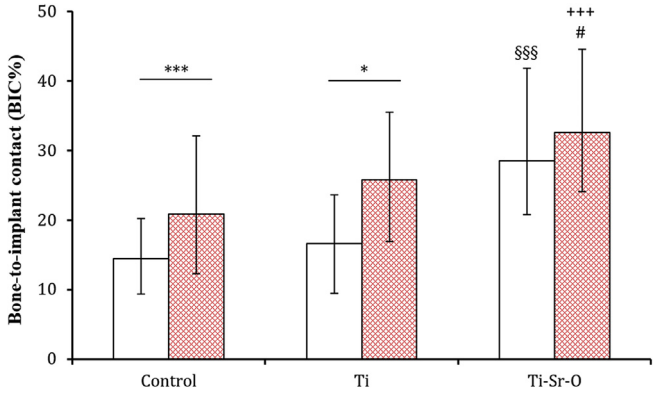

Fig. 9. BIC% after two (white column) and twelve (red squared column) weeks post-operatively. Significant differences between the two time intervals are marked with *($P < 0.05$) and ***($P < 0.001$). Significant differences of Ti-Sr-O to Ti and Control within the two-week observation period are marked with §§§($P < 0.001$), within the twelve-week time frame with $^{\#}$($P < 0.05$) compared to Ti and $^{+++}$($P < 0.001$) referring to Control, respectively. (For interpretation of the references to colour in this figure legend, the reader is referred to the web version of this article.)

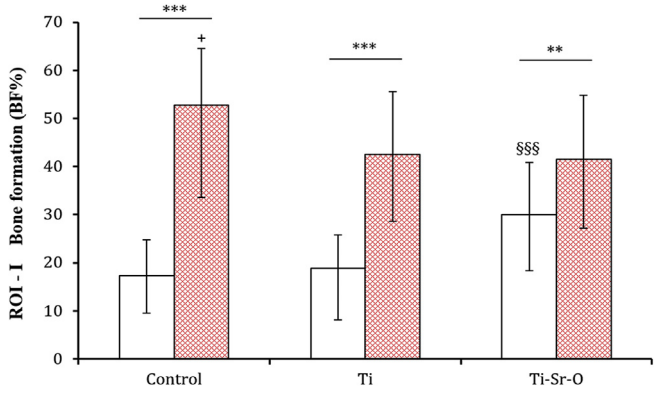

Fig. 10. BF% ROI-I after two (white column) and twelve (red squared column) weeks post-operatively. Significant differences between the two time intervals are marked with **($P < 0.01$) and ***($P < 0.001$). Significant differences of Ti-Sr-O compared to Ti and Control within the two-week observation period are marked with §§§($P < 0.001$), of Control compared to Ti and Ti-Sr-O within the twelve-week observation with $^{+}$($P < 0.05$). (For interpretation of the references to colour in this figure legend, the reader is referred to the web version of this article.)

face. This liberation shortly after implant insertion with values in the μg-range is improbable to affect systemic bone metabolism since systemic effects achieved with two grams SrRan per day for medical osteoporotic treatment in humans result in significantly higher strontium serum levels [54] than the described Ti-Sr-O surface [55]. Even so, these data has to be interpreted cautiously for obvious reasons of different physiological conditions in humans and rabbits. Calcium representing a crucial factor in bone metabolism was not significantly affected in the evaluated time frame with stable serum concentrations ranging from 2.5 to 3.5 mmol/L. Histological data in synopsis with spectrometry analysis therefore does not imply a systemic effect. However, a potential influence on the Ti implant in the other femur cannot be entirely precluded since bone formation for the Ti-Sr-O and Ti groups in both ROI-I and II behaved similarly while exceeding bone formation, relative to the Control group after twelve weeks and should be subjected to further studies.

μ-CT data revealed resembling trends compared to histomorphometrical analysis with no statistical significance, though. The loss of information during the histological sawing and grinding process could possibly could lead to uncertain results, which was also reported earlier [56,57]. In the current study cutting sections were applied in the center of the implant at the maximum diameter, gaining two slides per implant which could also contribute to the lack of significance since Bernhardt et al. proposed manufacturing of three to four histological sections [58]. Furthermore, μ-CT analysis is potentially limited by metal artifacts and different mineralization stages of surrounding bone [59]. However, as

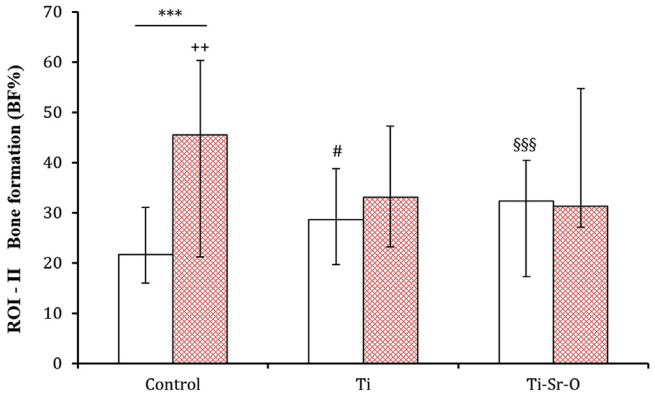

Fig. 11. BF% ROI-II after two (white column) and twelve (red squared column) weeks post-operatively. Significant differences between the two time intervals are marked with ***($P < 0.001$). Ti-Sr-O values in the two week observation period revealed disparities referring to Control §§§($P < 0.001$) while no significance to Ti was observed. Differences between Ti and Control are marked with $^{\#}$($P < 0.05$); within the twelve week observation period Control showed significance difference compared to Ti and Ti-Sr-O $^{++}$($P < 0.01$). (For interpretation of the references to colour in this figure legend, the reader is referred to the web version of this article.)

non-destructive evaluation, micro-computed tomography is a desirable method for measuring bone parameters. Nonetheless, gaining information on osseointegration should be employed carefully due to several drawbacks [59]. According to Bernhardt et al. up to 35% difference between μ-CT and histology can be detected [58] while Liu et al. even report on a 48 μm exclusion zone for evaluation of BIC% because of a so-called metal-induced artefact zone [57]. This represents a major concern that should be further addressed in future evaluations with proper preparation of scans and histological sections for appropriate matching of associated slides. The reported evaluation of bone formation in defined regions of interest should be subjected to push-out and torque tests to evaluate a correlation between increased bone apposition in surrounding *peri*-implant areas and a potentially enhanced mechanical stability. With respect to stimulation of bone response to the strontium functionalized surface, it is noticeable that ROI-II and more importantly BIC% revealed similar results in the observed time intervals which is understood as acceleration of osseointegration with comparable results even after an extended healing period of an additional ten weeks.

To our knowledge, this is the first report of a magnetron sputtered functionalized surface with *in vivo* investigations on early and late osseointegration stages with evaluation of potential systemic effects of liberated strontium. It was observed, that local administration of strontium from the implant interface shortens the healing period significantly. Future experiments should consider benchmarking the examined surface modification against established surface modifications in dental and orthopedic implantology.

The investigated functionalized surface showing sustained strontium release characteristics could possibly serve as a potential candidate for future surface adjustments in relation to both orthopedic and dental implant devices. The results from this study suggest that strontium-doped surfaces with tailored release profiles could have advantages referring to enhanced fixation for early loading and acceleration of the osseointegration process.

5. Conclusion

This study reports on the acquainted anabolic effect of strontium-modified implants in a rabbit femur model evaluating early and late osseointegration stages.

A Ti-Sr-O coating was deposited onto Ti implants by non-reactive DC magnetron sputtering using an industrial-scale system. *In vitro* analysis of functionalized implants showed a nanostructured surface (SEM), releasing the majority of strontium within the first two weeks (ICP-AES). This local release of strontium caused by Ti-Sr-O functionalization showed beneficial effects on osseointegration parameters in the two-week observation period. μ-CT data did not show significant differences while histologically evaluated experimental groups revealed significant differences with respect to bone-to-implant contact. Additionally, analyzed blood serum levels (AAS) did not indicate systemic effects as strontium and calcium labels were stable over a 28-day observation period.

Conclusively, the present experiments demonstrated that a magnetron sputtered functionalized titanium surface showing sustained release of strontium could improve early osseointegration and therefore serve as a potential candidate for modification of surfaces in orthopedic and dental implantology.

Acknowledgement

We like to acknowledge Prof. DDr. Michael Rasse for his input in numerous discussions to improve this manuscript. The authors would like to thank DDr. Tobias Petz and Dr. Anne Grote for their contribution, Shasta Pelzer for preparing histological sections and Dr. Peter Hald, Department of Chemistry at Aarhus University, for access to the ICP-AES equipment.

Funding

The project has been supported by the Innovation Fund Denmark through the project "Strontium functionalized titanium implants" and by the Danish Agency for Science, Technology and Innovation through a mobility scholarship.

Disclosure

The authors report no conflicts of interest.

Appendix A. Supplementary data

Supplementary data associated with this article can be found, in the online version, at https://doi.org/10.1016/j.actbio.2018.01.049.

References

[1] H. Malchau, P. Herberts, T. Eisler, G. Garellick, P. Soderman, The swedish total hip replacement register, J. Bone Joint Surg. Am. 2 (2002) 2–20.
[2] V. Chappuis, R. Buser, U. Bragger, M.M. Bornstein, G.E. Salvi, D. Buser, Long-term outcomes of dental implants with a titanium plasma-sprayed surface: a 20-year prospective case series study in partially edentulous patients, Clin. Implant Dent. Relat. Res. 15 (2013) 780–790.
[3] F. Schwarz, M. Wieland, Z. Schwartz, G. Zhao, F. Rupp, J. Geis-Gerstorfer, A. Schedle, N. Broggini, M.M. Bornstein, D. Buser, S.J. Ferguson, J. Becker, B.D. Boyan, D.L. Cochran, Potential of chemically modified hydrophilic surface characteristics to support tissue integration of titanium dental implants, J. Biomed. Mater. Res. B Appl. Biomater. 88 (2009) 544–557.
[4] J.W. Park, J.H. Jang, C.S. Lee, T. Hanawa, Osteoconductivity of hydrophilic microstructured titanium implants with phosphate ion chemistry, Acta Biomater. 5 (2009) 2311–2321.
[5] A. Wennerberg, T. Albrektsson, On implant surfaces: a review of current knowledge and opinions, Int. J. Oral Maxillofac. Implants 25 (2010) 63–74.
[6] H. Yazici, H. Fong, B. Wilson, E.E. Oren, F.A. Amos, H. Zhang, J.S. Evans, M.L. Snead, M. Sarikaya, C. Tamerler, Biological response on a titanium implant-grade surface functionalized with modular peptides, Acta Biomater. 9 (2013) 5341–5352.
[7] R. Smeets, B. Stadlinger, F. Schwarz, B. Beck-Broichsitter, O. Jung, C. Precht, F. Kloss, A. Gröbe, M. Heiland, T. Ebker, Impact of dental implant surface modifications on osseointegration, Biomed. Res. Int. 6285620 (2016) 11.
[8] T. Moutinho, Reviewing the data on survival rates of stems and cups in total hip replacement, J. Bone Joint Surg. Am. 85-A (5) (2003) 970. author reply 970.
[9] F. Rupp, L. Scheideler, N. Olshanska, M. de Wild, M. Wieland, J. Geis-Gerstorfer, Enhancing surface free energy and hydrophilicity through chemical

modification of microstructured titanium implant surfaces, J. Biomed. Mater. Res. A 76 (2006) 323–334.
[10] G.I. Benic, J. Mir-Mari, C.H. Hammerle, Loading protocols for single-implant crowns: a systematic review and meta-analysis, Int. J. Oral Maxillofac. Implants 29 (2014) 222–238.
[11] F.R. Kloss, S. Singh, O. Hachl, J. Rentenberger, T. Auberger, A. Kraft, G. Klima, T. Mitterlechner, D. Steinmüller-Nethl, B. Lethaus, M. Rasse, G. Lepperdinger, R. Gassner, BMP-2 immobilized on nanocrystalline diamond-coated titanium screws; demonstration of osteoinductive properties in irradiated bone, Head Neck 35 (2013) 235–241.
[12] F. Fontana, I. Rocchietta, A. Addis, P. Schupbach, G. Zanotti, M. Simion, Effects of a calcium phosphate coating on the osseointegration of endosseous implants in a rabbit model, Clin. Oral Implants Res. 22 (2011) 760–766.
[13] S. Galli, Y. Naito, J. Karlsson, W. He, I. Miyamoto, Y. Xue, M. Andersson, K. Mustafa, A. Wennerberg, R. Jimbo, Local release of magnesium from mesoporous TiO2 coatings stimulates the peri-implant expression of osteogenic markers and improves osteoconductivity in vivo, Acta Biomater. 10 (2014) 5193–5201.
[14] O.Z. Andersen, V. Offermanns, M. Sillassen, K.P. Almtoft, I.H. Andersen, S. Sorensen, C.S. Jeppesen, D.C. Kraft, J. Bøttiger, M. Rasse, F. Kloss, M. Foss, Accelerated bone ingrowth by local delivery of strontium from surface functionalized titanium implants, Biomaterials 34 (2013) 5883–5890.
[15] R.K. Schenk, D. Buser, Osseointegration: a reality, Periodontology 1998 (17) (2000) 22–35.
[16] G. Mendonca, D.B. Mendonca, F.J. Aragao, L.F. Cooper, Advancing dental implant surface technology–from micron- to nanotopography, Biomaterials 29 (2008) 3822–3835.
[17] M. Adam, C. Ganz, W. Xu, H.R. Sarajian, W. Gotz, T. Gerber, In vivo and in vitro investigations of a nanostructured coating material - a preclinical study, Int. J. Nanomed. 9 (2014) 975–984.
[18] L. Zhao, H. Wang, K. Huo, X. Zhang, W. Wang, Y. Zhang, Z. Wu, P.K. Chu, The osteogenic activity of strontium loaded titania nanotube arrays on titanium substrates, Biomaterials 34 (2013) 19–29.
[19] Y. Li, Y. Qi, Q. Gao, Q. Niu, M. Shen, Q. Fu, K. Hu, L. Kong, Effects of a micro/nano rough strontium-loaded surface on osseointegration, Int. J. Nanomed. 10 (2015) 4549–4563.
[20] H. Cheng, W. Xiong, Z. Fang, H. Guan, W. Wu, Y. Li, Y. Zhang, M.M. Alvarez, B. Gao, K. Huo, J. Xu, N. Xu, C. Zhang, J. Fu, A. Khademhosseini, F. Li, Strontium (Sr) and silver (Ag) loaded nanotubular structures with combined osteoinductive and antimicrobial activities, Acta Biomater. 31 (2016) 388–400.
[21] G. Bhardwaj, T.J. Webster, Reduced bacterial growth and increased osteoblast proliferation on titanium with a nanophase TiO2 surface treatment, Int. J. Nanomed. 12 (2017) 363–369.
[22] D. Karazisis, S. Petronis, H. Agheli, L. Emanuelsson, B. Norlindh, A. Johansson, L. Rasmusson, P. Thomsen, O. Omar, The influence of controlled surface nanotopography on the early biological events of osseointegration, Acta Biomater. 53 (2017) 559–571.
[23] F.E. McCaslin, J.M. Janes, The effect of strontium lactate in the treatment of osteoporosis, Proc. Staff Meet. Mayo Clin. 34 (1959) 329–334.
[24] P.J. Meunier, C. Roux, E. Seeman, S. Ortolani, J.E. Badurski, T.D. Spector, J. Cannata, A. Balogh, E.M. Lemmel, S. Pors-Nielsen, R. Rizzoli, H.K. Genant, J.Y. Reginster, The effects of strontium ranelate on the risk of vertebral fracture in women with postmenopausal osteoporosis, N. Engl. J. Med. 350 (2004) 459–468.
[25] J.Y. Reginster, E. Seeman, M.C. De Vernejoul, S. Adami, J. Compston, C. Phenekos, J.P. Devogelaer, M.D. Curiel, A. Sawicki, S. Goemaere, O.H. Sorensen, D. Felsenberg, P.J. Meunier, Strontium ranelate reduces the risk of nonvertebral fractures in postmenopausal women with osteoporosis: Treatment of Peripheral Osteoporosis (TROPOS) study, J. Clin. Endocrinol. Metabo. 90 (2005) 2816–2822.
[26] M. Audran, F.J. Jakob, S. Palacios, M.L. Brandi, H. Broll, N.A. Hamdy, E.V. McCloesky, A large prospective European cohort study of patients treated with strontium ranelate and followed up over 3 years, Rheumatol. Int. 33 (9) (2013 Sep) 2231–2239.
[27] Z. Saidak, P.J. Marie, Strontium signaling: molecular mechanisms and therapeutic implications in osteoporosis, Pharmacol. Ther. 136 (2012) 216–226.
[28] Z. Saidak, E. Hay, C. Marty, A. Barbara, P.J. Marie, Strontium ranelate rebalances bone marrow adipogenesis and osteoblastogenesis in senescent osteopenic mice through NFATc/Maf and Wnt signaling, Aging Cell 11 (2012) 467–474.
[29] E. Gentleman, Y.C. Fredholm, G. Jell, N. Lotfibakhshaiesh, M.D. O'Donnell, R.G. Hill, M.M. Stevens, The effects of strontium-substituted bioactive glasses on osteoblasts and osteoclasts in vitro, Biomaterials 31 (2010) 3949–3956.
[30] C. Wu, W. Fan, M. Gelinsky, Y. Xiao, P. Simon, R. Schulze, T. Doert, Y. Luo, G. Cuniberti, Bioactive SrO-SiO2 glass with well-ordered mesopores: characterization, physiochemistry and biological properties, Acta Biomater. 7 (2011) 1797–1806.
[31] Y. Zhu, M. Zhu, X. He, J. Zhang, C. Tao, Substitutions of strontium in mesoporous calcium silicate and their physicochemical and biological properties, Acta Biomater. 9 (2013) 6723–6731.
[32] U. Thormann, S. Ray, U. Sommer, T. Elkhassawna, T. Rehling, M. Hundgeburth, A. Henß, M. Rohnke, J. Janek, K.S. Lips, C. Heiss, G. Schlewitz, G. Szalay, M. Schumacher, M. Gelinsky, R. Schnettler, V. Alt, Bone formation induced by strontium modified calcium phosphate cement in critical-size metaphyseal fracture defects in ovariectomized rats, Biomaterials 34 (2013) 8589–8598.
[33] V. Offermanns, O.Z. Andersen, G. Falkensammer, I.H. Andersen, K.P. Almtoft, S. Sorensen, M. Sillassen, C.S. Jeppesen, M. Rasse, M. Foss, F. Kloss, Enhanced osseointegration of endosseous implants by predictable sustained release properties of strontium, J. Biomed. Mater. Res. B Appl. Biomater. 25 (2014) 33279.
[34] V. Offermanns, O.Z. Andersen, G. Riede, I.H. Andersen, K.P. Almtoft, S. Sorensen, M. Sillassen, C.S. Jeppesen, M. Rasse, M. Foss, F. Kloss, Bone regenerating effect of surface-functionalized titanium implants with sustained-release characteristics of strontium in ovariectomized rats, Int. J. Nanomed. 11 (2016) 2431–2442.
[35] S. Rupprecht, A. Bloch-Birkholz, B. Lethaus, S. Rosiwal, F.W. Neukam, A. Schlegel, The bone-metal interface of defect and press-fit ingrowth of microwave plasma-chemical vapor deposition implants in the rabbit model, Clin. Oral Implants Res. 16 (2005) 98–104.
[36] M. Sillassen, C.S. Jeppesen, O.Z. Andersen, K.P. Almtoft, S. Sørensen, I.H. Andersen, L.P. Nielsen, M. Foss, J. Bøttiger, Controlled Sr release from Ti–Sr–O films deposited by non-reactive magnetron sputtering in an industrial setup, Surf. Coat. Technol. 252 (2014) 56–63.
[37] C. Kilkenny, W.J. Browne, I.C. Cuthill, M. Emerson, D.G. Altman, Improving bioscience research reporting: the ARRIVE guidelines for reporting animal research, PLoS Biol. 8 (2010) e1000412.
[38] A. Dülsner, R. Hack, C. Krüger, M. Pils, K. Scherer, B. Schmelting, M. Schmidt, H. Weinert, T. Jourdan, http://www.gv-solas.de/fileadmin/user_upload/pdf_publikation/Tierschutzbeauftragte/tie_blutentnahme17.pdf. In: GV-SOLAS 2017. pp. 11–18.
[39] K. Donath, G. Breuner, A method for the study of undecalcified bones and teeth with attached soft tissues. The sage-schliff (sawing and grinding) technique, J. Oral Pathol. 11 (1982) 318–326.
[40] J.Y. Reginster, R. Deroisy, M. Dougados, I. Jupsin, J. Colette, C. Roux, Prevention of early postmenopausal bone loss by strontium ranelate: the randomized, two-year, double-masked, dose-ranging, placebo-controlled PREVOS trial, Osteoporosis Int. 13 (2002) 925–931.
[41] L. Maimoun, T.C. Brennan, I. Badoud, V. Dubois-Ferriere, R. Rizzoli, P. Ammann, Strontium ranelate improves implant osseointegration, Bone 46 (2010) 1436–1441.
[42] Y. Li, X. Li, G. Song, K. Chen, G. Yin, J. Hu, Effects of strontium ranelate on osseointegration of titanium implant in osteoporotic rats, Clin. Oral Implants Res. 23 (2012) 1038–1044.
[43] T. Albrektsson, P.I. Branemark, H.A. Hansson, J. Lindstrom, Osseointegrated titanium implants. Requirements for ensuring a long-lasting, direct bone-to-implant anchorage in man, Acta Orthop. Scand. 52 (1981) 155–170.
[44] D. Buser, N. Broggini, M. Wieland, R.K. Schenk, A.J. Denzer, D.L. Cochran, B. Hoffmann, A. Lussi, S.G. Steinemann, Enhanced bone apposition to a chemically modified SLA titanium surface, J. Dent Res. 83 (2004) 529–533.
[45] B. Stadlinger, P. Korn, N. Todtmann, U. Eckelt, U. Range, A. Burki, S.J. Ferguson, I. Kramer, A. Kautz, M. Schnabelrauch, M. Kneissel, F. Schlottig, Osseointegration of biochemically modified implants in an osteoporosis rodent model, Eur. Cell Mater. 25 (2013) 326–340. discussion 39-40.
[46] M.J. Bolland, A. Grey, Ten years too long: strontium ranelate, cardiac events, and the European Medicines Agency, BMJ 354 (2016) i5109.
[47] P. Watts, P. Howe, Strontium and strontium compounds, in: World Health Organization (Ed.), Concise International Chemical Assessment Document, 77, 2010.
[48] D.S. Brauer, N. Karpukhina, G. Kedia, A. Bhat, R.V. Law, I. Radecka, R.G. Hill, Bactericidal strontium-releasing injectable bone cements based on bioactive glasses, J. R Soc. Interface 24 (2012) 24.
[49] C. Riedel, E.A. Zimmermann, J. Zustin, M. Niecke, M. Amling, M. Grynpas, B. Busse, The incorporation of fluoride and strontium in hydroxyapatite affects the composition, structure, and mechanical properties of human cortical bone, J. Biomed. Mater. Res. A 105 (2017) 433–442.
[50] Y. Li, Q. Li, S. Zhu, E. Luo, J. Li, G. Feng, Y. Liao, J. Hu, The effect of strontium-substituted hydroxyapatite coating on implant fixation in ovariectomized rats, Biomaterials 31 (2010) 9006–9014.
[51] B.G. Zhang, D.E. Myers, G.G. Wallace, M. Brandt, P.F. Choong, Bioactive coatings for orthopaedic implants-recent trends in development of implant coatings, Int. J. Mol. Sci. 15 (2014) 11878–11921.
[52] E.A. Abou Neel, A. Aljabo, A. Strange, S. Ibrahim, M. Coathup, A.M. Young, L. Bozec, V. Mudera, Demineralization-remineralization dynamics in teeth and bone, Int. J. Nanomed. 11 (2016) 4743–4763.
[53] A.I. Pearce, R.G. Richards, S. Milz, E. Schneider, S.G. Pearce, Animal models for implant biomaterial research in bone: a review, Eur. Cell Mater. 13 (2007) 1–10.
[54] EMA. http://www.ema.europa.eu/docs/en_GB/document_library/EPAR_-_Scientific_Discussion/human/000560/WC500045522.pdf. 2005: pp. 1–23.
[55] J.M. Kaufman, M. Audran, G. Bianchi, V. Braga, M. Diaz-Curiel, R.M. Francis, S. Goemaere, R. Josse, S. Palacios, J.D. Ringe, D. Felsenberg, S. Boonen, Efficacy and safety of strontium ranelate in the treatment of osteoporosis in men, J. Clin. Endocrinol. Metabolism 98 (2013) 592–601.
[56] L. Sennerby, A. Wennerberg, F. Pasop, A new microtomographic technique for non-invasive evaluation of the bone structure around implants, Clin. Oral Implants Res. 12 (2001) 91–94.
[57] S. Liu, J. Broucek, A.S. Virdi, D.R. Sumner, Limitations of using micro-computed tomography to predict bone-implant contact and mechanical fixation, J. Microsc. 245 (2012) 34–42.
[58] R. Bernhardt, E. Kuhlisch, M.C. Schulz, U. Eckelt, B. Stadlinger, Comparison of bone-implant contact and bone-implant volume between 2D-histological sections and 3D-SRmicroCT slices, Eur. Cell Mater. 23 (2012) 237–247.
[59] C. von Wilmowsky, T. Moest, E. Nkenke, F. Stelzle, K.A. Schlegel, Implants in bone: part II. Research on implant osseointegration: material testing, mechanical testing, imaging and histoanalytical methods, Oral Maxillofac. Surg. 18 (2014) 355–372.